Received: 16 February 2024 | Revised: 19 March 2024 | Accepted: 22 March 2024

DOI: 10.1002/aoc.7483

RESEARCH ARTICLE

Applied Organometallic Chemistry WILEY

Amino acid-decorated mesoporous silica nanoparticles loaded with titanocene derivatives for targeted anticancer studies

Michael Aondona Iorhemba[1,2,3] | **Karina Ovejero-Paredes**[4,5] | **Diana Díaz-García**[1] | **Victoria García-Almodóvar**[1] | **Sulaiman Ola Idris**[2] | **Gideon Adamu Shallangwa**[2] | **Ibrahim Abdulkadir**[2] | **José M. Méndez-Arriaga**[1] | **Sanjiv Prashar**[1] | **Marco Filice**[4,5] | **Santiago Gómez-Ruiz**[1]

[1]COMET-NANO Group, Departamento de Biología y Geología, Física y Química Inorgánica, E.S.C.E.T., Universidad Rey Juan Carlos, Madrid, Spain

[2]Department of Chemistry, Faculty of Physical Sciences, Ahmadu Bello University, Zaria, Nigeria

[3]Department of Chemistry, College of Physical Sciences, Federal University of Agriculture, Makurdi, Nigeria

[4]Nanobiotechnology for Life Sciences Group, Department of Chemistry in Pharmaceutical Sciences, Faculty of Pharmacy, Universidad Complutense de Madrid (UCM), Madrid, Spain

[5]Microscopy and Dynamic Imaging Unit, Fundación Centro Nacional de Investigaciones Cardiovasculares Carlos III (CNIC), Madrid, Spain

Correspondence
Marco Filice, Nanobiotechnology for Life Sciences Group, Department of Chemistry in Pharmaceutical Sciences, Faculty of Pharmacy, Universidad Complutense de Madrid (UCM), Plaza Ramón y Cajal s/n, E-28040 Madrid, Spain.
Email: mfilice@ucm.es

Santiago Gómez-Ruiz, COMET-NANO Group, Departamento de Biología y Geología, Física y Química Inorgánica, E.S.C.E.T., Universidad Rey Juan Carlos, Calle Tulipán s/n, E-28933, Móstoles, Madrid, Spain.
Email: santiago.gomez@urjc.es

Funding information
Ministerio de Ciencia, Innovación y Universidades, Grant/Award Numbers: PID2022-136417NB-I00, RED2022-134091-T, CPP2022-009952; Tertiary Education Trust Fund, Grant/Award Number: MAIFellowship; Universidad Rey Juan Carlos, Grant/Award Number: M3271; Instituto de Salud Carlos III

Nanostructured materials possess promising potential for cancer therapy through precise adjustment of their functionalization and physicochemical attributes. This study primarily focuses on the synthesis and characterization of mesoporous silica nanoparticles (MSN) that are functionalized with titanocene dichloride (a therapeutic agent) and one of several amino acids—cysteine, captopril, penicillamine, or methionine—utilizing 3-aminopropyltriethoxysilane (AP) as a linker. This synthesis yielded four innovative metallodrug-functionalized nanostructured materials (MSN-AP-Cys-Ti, MSN-AP-Cap-Ti, MSN-AP-Pen-Ti, and MSN-AP-Met-Ti), meticulously characterized using diverse analytical techniques such as X-ray diffraction (XRD), X-ray fluorescence (XRF), diffuse reflectance ultraviolet–visible (DR UV–Vis), Fourier transform infrared (FTIR), solid-state nuclear magnetic resonance (NMR) spectroscopy, and transmission electron microscopy (TEM). The textural properties of the nanomaterials post-functionalization displayed slight modifications, confirming the successful integration of the therapeutic agents. Evaluation of cytotoxicity in the breast cancer cell line MDA-MB-231, with the healthy cell line Hek-293T as control via MTT assays, revealed the active nature of the functionalized silica-based materials. The viability of both cell lines indicated a concentration-dependent response to the materials. Among the tested systems, cysteine and captopril

exhibited the highest activity concerning IC_{50} relative to material concentration. The enhanced biological activity of higher functionalized nanosystems suggests a favorable cell internalization facilitated by the amino acid fragment. Additionally, qualitative DNA binding studies hinted at potential DNA adsorption on the surface of the metallodrug-functionalized nanomaterials, forming DNA adducts where a strand of DNA covalently bonds to the metallodrug moiety. This was deduced from the hypsochromic shift in absorbance of the characteristic π–π^* and n–π^* transitions in DNA, which occurred from 1.01 to 0.76 and 1.26–0.19 following drug (MSN-AP-Cap-Ti) interaction.

KEYWORDS

amino acid, anticancer, cell viability, cytotoxicity, mesoporous silica nanoparticles, titanocene dichloride

1 | INTRODUCTION

Cancer remains a pervasive global health challenge, claiming nearly 10 million lives in 2020 and standing as the second leading cause of mortality after cardiovascular diseases. In that year, the most prevalent cancer-related fatalities encompassed lung (1.80 million deaths), colon and rectum (935,000 deaths), liver (830,000 deaths), stomach (769,000 deaths), and breast cancer (685,000 deaths). Alarmingly, cancer prevalence is projected to soar by approximately 70% in developing countries over the next decade.[1–3] Among these, breast cancer emerges as the most frequently diagnosed life-threatening cancer in women, causing around 570,000 deaths in 2015, with over 1.5 million new cases reported annually worldwide.[4–6]

The staggering toll of cancer has galvanized significant efforts toward discovering new treatments and enhancing conventional drugs through innovative formulations.

Presently, cancer treatments predominantly rely on radiotherapy, chemotherapy, and biological therapies.[7] Platinum-based metal drugs have long been a mainstay in chemotherapy, effectively curbing the unchecked proliferation of cancer cells.[8,9] However, their use is marred by inherent drawbacks—ranging from toxicity and low stability in physiological conditions to inadequate tumor-targeting strategies.[2,10]

To overcome these challenges, extensive research has pivoted toward alternative metal-based drugs[10,11] and metallodrug-functionalized systems. These systems aim to achieve controlled drug loading, targeted delivery, and selective release to bolster their therapeutic potential.[2,12,13] Although the structure of metallodrugs typically correlates with cytotoxicity, it is established that their structure undergoes transformation during transportation to cells, leading to alterations in their behavior akin to prodrugs.[14] This scenario has spurred interest in encapsulating these active species for protected delivery to cancer cells, prompting widespread exploration of various nanostructured systems in both in vitro and in vivo anticancer chemotherapy.[2,12]

Amino acids and their derivatives have demonstrated massive importance in the search for new chemotherapeutic agents. For instance, captopril has shown promising results as an anticancer agent in both in vitro and in vivo investigations, particularly in inhibiting the growth of human lung tumors.[15] Penicillamine has also been found to increase the therapeutic efficacy of platinum drugs in oxaliplatin-resistant tumors.[16] Additionally, cysteine has been documented for its cancer-marking and -targeting ability.[17] Thus, the notion of incorporating amino acids into silica-based materials functionalized with cytotoxic titanocene fragments emerged as a promising avenue for crafting novel nanoformulations with therapeutic potential.[2,12]

In recent years, mesoporous silica nanoparticles have gained prominence as versatile drug delivery systems and theranostic probes because of inherent qualities like stability, tunable porosity, biocompatibility, and facile functionalization with biologically relevant molecules.[18–20] Modified MSNs exhibit favorable attributes for targeted internalization, stimuli-responsive, prolonged circulation, and contrast imaging.[21] For instance, folate-conjugated MSNs exhibit high efficiency in internalizing into cancer cells, underscoring the pivotal role of surface chemical functionality in cellular uptake.[22]

This study aims to incorporate various amino acids into silica-based materials functionalized with metallodrugs for in vitro antiproliferative studies against breast cancer cells (MDA-MB-231). Mesoporous silica nanoparticles were chosen for their high surface area, enabling optimal functionalization with biologically relevant fragments and a small particle size conducive to effective therapeutic action. Herein, we detail the synthesis and

characterization of four cytotoxic titanocene–amino acid functionalized nanostructured materials, assessing their in vitro antitumor activity through cytotoxicity analysis.

2 | MATERIALS AND METHODS

2.1 | Materials

The reagents used in the preparation of the starting material (MSN) were tetraethyl orthosilicate (TEOS, Sigma Aldrich) and hexadecyltrimethylammonium bromide (CTAB, Acros Organics) and sodium hydroxide (Scharlau), which were used as received, without further purification. The reagents used for the functionalization reactions, namely, L-cysteine, captopril, L-penicillamine, and L-methionine, were obtained from Sigma Aldrich. Also, 2-morpholinoethanesulphonic acid monohydrate (MES monohydrate), EDAC, N-hydroxysuccinamide (NHS), and 3-aminopropyltriethoxysilane (AP) were purchased from Sigma Aldrich and used directly without further purification.

Additionally, 3-mercaptopropyltriethoxysilane (MP) was purchased from Fluorochem Ltd. (Derbyshire, UK) and was well used as received. Titanocene dichloride [$Ti(\eta^5\text{-}C_5H_5)_2Cl_2$] was also a Sigma Aldrich product and used as received. The human breast carcinoma cell line (MDA-MB-231) and human embryonic kidney cell line (HEK-293T) were obtained from ATCC. DMEM-GlutaMAX was obtained from Gibco. DMEM-F12 and penicillin/streptomycin were obtained from Lonza. Non-essential amino acids and sodium pyruvate were obtained from Hyclone. Fetal bovine serum (FBS), phosphate-buffered saline (PBS), cisplatin dimethylthiazolyl-diphenyl-tetrazolium bromide (MTT reagent), fish sperm-deoxyribonucleic acid (FS-DNA), tris buffer, and dimethylsulfoxide (DMSO) were all Sigma Aldrich products used as received. Organic solvents employed were distilled from the appropriate drying agents and degassed before use.

2.2 | Synthetic methods

General remarks on the characterization of the materials, the DNA binding studies, and the cytotoxicity tests are given in the Supporting Information.

2.3 | Functionalization of MSN with different ligands

The synthesis of MSN and functionalization followed a modified procedure from our previous work.[23] For MSN-AP (1:1 MSN:AP weight ratio), 2 g of MSN underwent drying at 80°C under vacuum overnight. The dispersion of MSN in 40 mL of dry toluene involved adding 2.10 mL (9.03 mmol) of 3-aminopropyltriethoxy silane and stirring the mixture at 110°C for 24 h. The resultant solid underwent centrifugation, washing with toluene and diethyl ether, and drying at 75°C.

For MSN-AP-Cys (Scheme 1) and in order to obtain 50% theoretical incorporation of cysteine, 1.16 g (6.03 mmol) of *N*-(3-dimethylaminopropyl)-*N*′-ethylcarbodiimide hydrochloride (EDAC) was added to a 60-mL 2-morpholinoethane sulfonic acid hydrate (MES) buffer solution in a glass bottle, followed by the addition of 1.74 g (15.08 mmol) of *N*-hydroxysuccinimide (NHS). The reaction was allowed to stir for 5 min at room temperature. Then, 0.6 g (4.95 mmol) of cysteine was added during continuous stirring for another 15 min followed by the addition of 1.20 g of MSN-AP. The reaction was kept under vigorous stirring at 50°C for an additional 4 h and then allowed to cool to room temperature. The resultant slurry was centrifuged at 3703 g for 10 min. The solid fraction was washed with Milli-Q water and ethanol and dried in an oven at 80°C overnight.

The same protocol for the captopril, penicillamine, and cysteine was followed to prepare MSN-AP-Cap and MSN-AP-Pen (Scheme 1).

For the synthesis of MSN-AP-Cys-Ti, 200 mg of MSN-AP-Cys and 6.25 mg of [$Ti(\eta^5\text{-}C_5H_5)_2Cl_2$] (0.025 mmol, considering that MSN-AP-Cys has 0.402% wt. S, corresponding to a 1:1 ratio Ti:S) were dispersed in 30 mL of dry toluene and 7.00 μL of triethyl amine (NEt_3, 0.058 mmol). The mixture was stirred for 24 h at 110°C. Subsequently, the mixture was centrifuged at 3703 g for 10 min, and the resulting isolated solid was washed with toluene and ethanol and dried overnight in an oven at 75°C.

Using the same procedure for the synthesis of MSN-AP-Cap-Ti, the following quantities were used: 200 mg of MSN-AP-Cap, 10.95 mg of [$Ti(\eta^5\text{-}C_5H_5)_2Cl_2$] (0.044 mmol), and 12.30 μL of NEt_3 (0.088 mmol). In addition, for the preparation of MSN-AP-Pen-Ti, the following quantities were used: 200 mg of MSN-AP-Pen, 7.82 mg of [$Ti(\eta\text{-}C_5H_5)_2Cl_2$] (0.031 mmol), and 8.65 μL of NEt_3 (0.062 mmol).

2.4 | Synthesis of [$Ti(\eta^5\text{-}C_5H_5)_2\{SCH_2CH_2CH_2Si(OEt)_3\}Cl$]

A solution of [$Ti(\eta^5\text{-}C_5H_5)_2Cl_2$] (104 mg, 0.418 mmol) (to obtain a theoretical level of 10% Ti/SiO_2) in 30 mL of dry toluene was prepared in a Schlenk tube and 106.93 μL of (3-mercaptopropyl) triethoxysilane

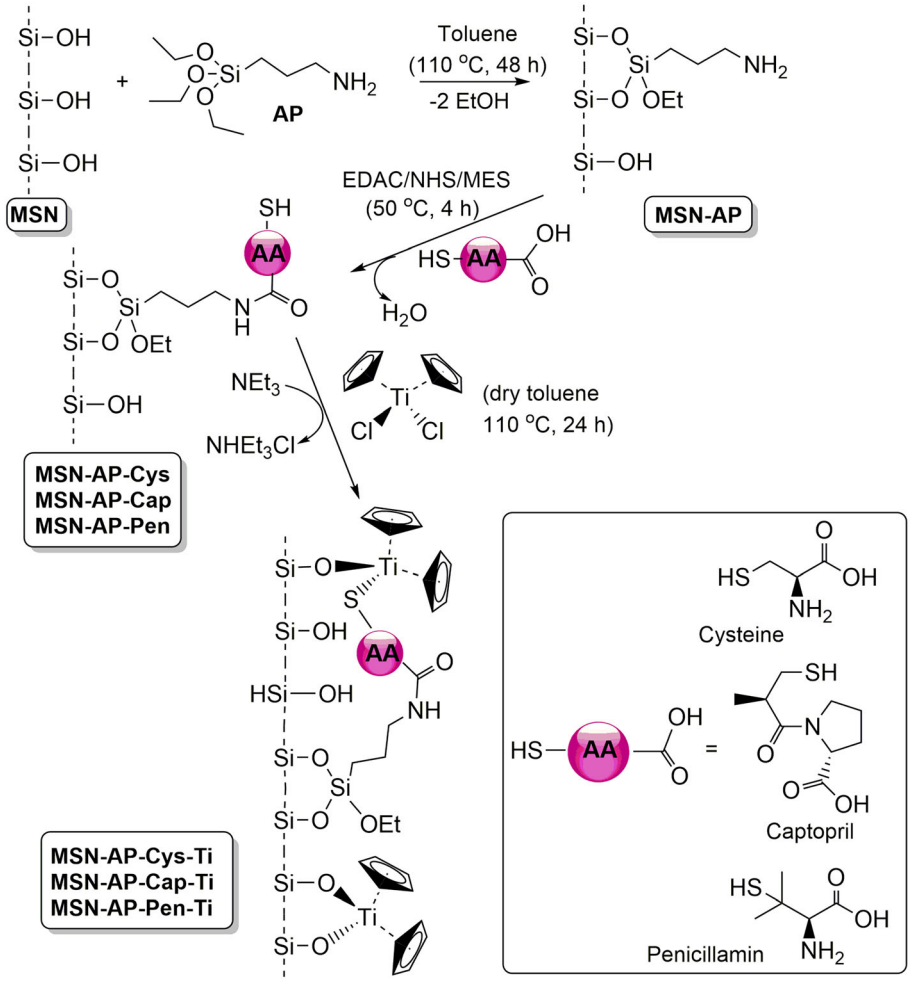

SCHEME 1 Synthesis of the titanocene-functionalized materials MSN-AP-Cys-Ti, MSN-AP-Cap-Ti, and MSN-AP-Pen-Ti.

(MP) (0.418 mmol) and 116.60 μL of NEt_3 (0.836 mmol) added. The mixture was stirred overnight at 110°C. The product, $[Ti(\eta^5\text{-}C_5H_5)_2\{SCH_2CH_2CH_2Si(OEt)_3\}Cl]$ (Scheme 2) was isolated by filtration and solvent removed in vacuo from the filtrate to yield the desired product.

2.5 | Preparation of MSN-AP-Met-Ti (Met = methionine)

The synthesis of MSN-AP-Met-Ti was carried out following a different protocol. This is because methionine does not possess a thiol (S–H) group in its molecule like the other amino acids but rather a thione (S–CH_3). Therefore, it is impossible to explore protonolysis in the synthesis of the final material incorporating methionine. Thus, to unify the environment of Ti in the final materials, 3-mercaptopropyltriethoxysilane (MP) was used to provide the Ti-S linkages. $[Ti(\eta^5\text{-}C_5H_5)_2\{SCH_2CH_2CH_2Si(OEt)_3\}Cl]$ was dissolved in 10 mL of dry toluene and mixed, under nitrogen atmosphere, with a dispersion of MSN-AP-Met (200 mg) in 20 mL of dry toluene (Scheme 2). The mixture was allowed to stir for 48 h at 110°C. Subsequently, the mixture was centrifuged at 3703 g for 10 min, and the resulting isolated solid was washed with toluene and ethanol and dried overnight in an oven at 80°C.

3 | RESULTS AND DISCUSSION

3.1 | Synthesis of titanocene-functionalized nanostructured silica-based materials

Amino acid-functionalized MSNs were prepared by the reaction of dehydrated MSN with 3-aminopropyltriethoxysilane in toluene and subsequent EDAC coupling reaction with the corresponding amino acid (cysteine, captopril, penicillamine, or methionine). Subsequently, the titanocene compound was incorporated into the materials containing cysteine, captopril, or penicillamine by reaction through the thiol group with the Ti-Cl bond of titanocene dichloride to give MSN-AP-Cys-Ti, MSN-AP-Cap-Ti, and MSN-AP-Pen-Ti (Scheme 1). On the other hand, the MSN-based system

SCHEME 2 Synthesis of MSN-AP-Met-Ti.

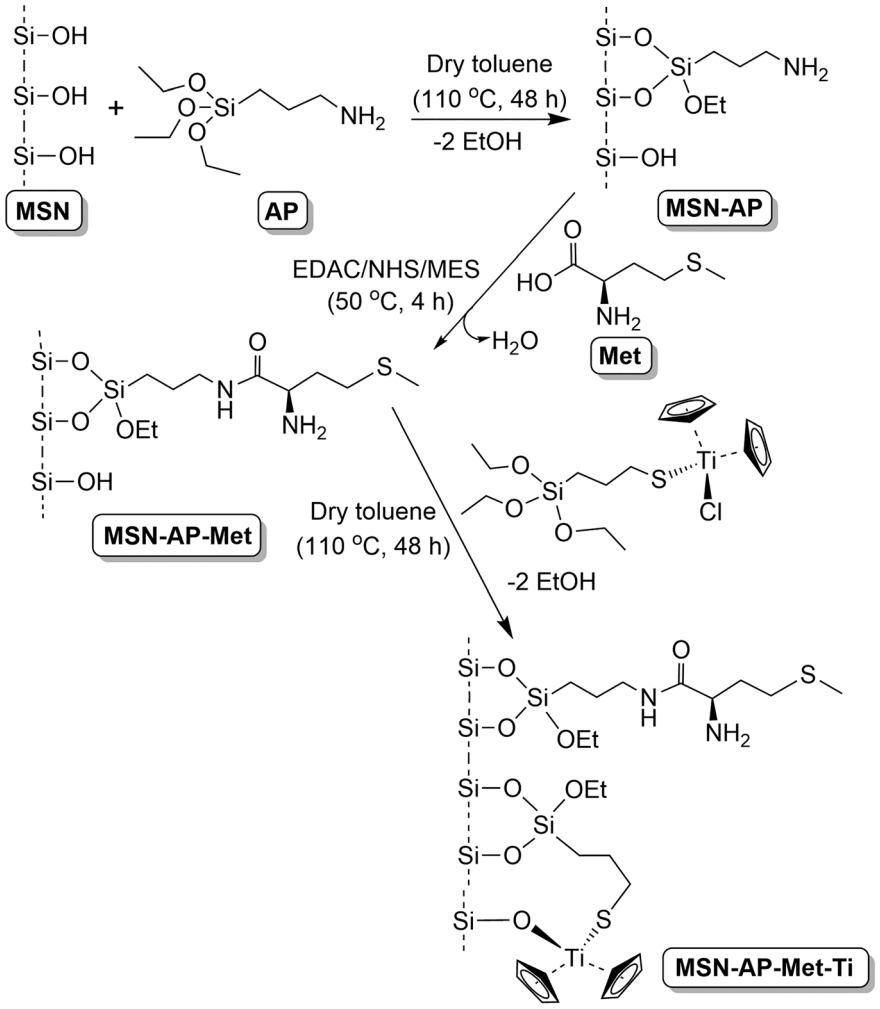

containing methionine was grafted with [Ti(η^5-C_5H_5)$_2${$SCH_2CH_2CH_2Si(OEt)_3$}Cl] to give MSN-AP-Met-Ti (Scheme 2). All the materials were characterized by different techniques to confirm the incorporation of both the amino acid fragment as well as the titanium-containing species.

3.2 | UV–visible measurements

The synthesized materials underwent characterization using diffused reflectance UV–Vis spectroscopy to ascertain the successful integration of diverse agents into the MSN matrix. Previous studies have validated the effectiveness of this method in confirming the inclusion of various ligands or metal complexes within nanostructured silica.[24,25] As depicted in Figure 1, the DR UV–Vis spectra of the materials revealed a discernible signal around 200–207 nm, indicative of the presence of AP ligands. This observation aligns with findings from similar materials incorporating analogous ligands, reaffirming successful integration within the structure.[23,24]

In addition, the incorporation of amino acid was deduced by the appearance of two bands at approximately 240 and 290 nm, associated with Ti-aa interaction.[26] Interestingly, the spectra of all the materials showed a shoulder appearing at approximately 390–410 nm, which could be assigned to ligand–metal charge transfer absorptions. Ordinarily, this band should be absent in the spectra of these materials considering that Ti (IV) is a d^0 electronic system. Its presence in the spectra of all the metallo-functionalized systems is due to the transfer of electrons from the electron-rich -S, -O, and Cp (Cp = η^5-C_5H_5) via the Ti-S, Ti-O, and Ti-Cp interactions in ligand–metal charge transfer (LMCT).

3.3 | FT-IR studies

The IR spectra of both the initial materials and the functionalized systems exhibit characteristic patterns associated with silica nanoparticles (Figure S1). The MSN spectra display a distinctive band at 3438 cm^{-1}, accompanied by another at 804 cm^{-1}, attributed to the vibrations

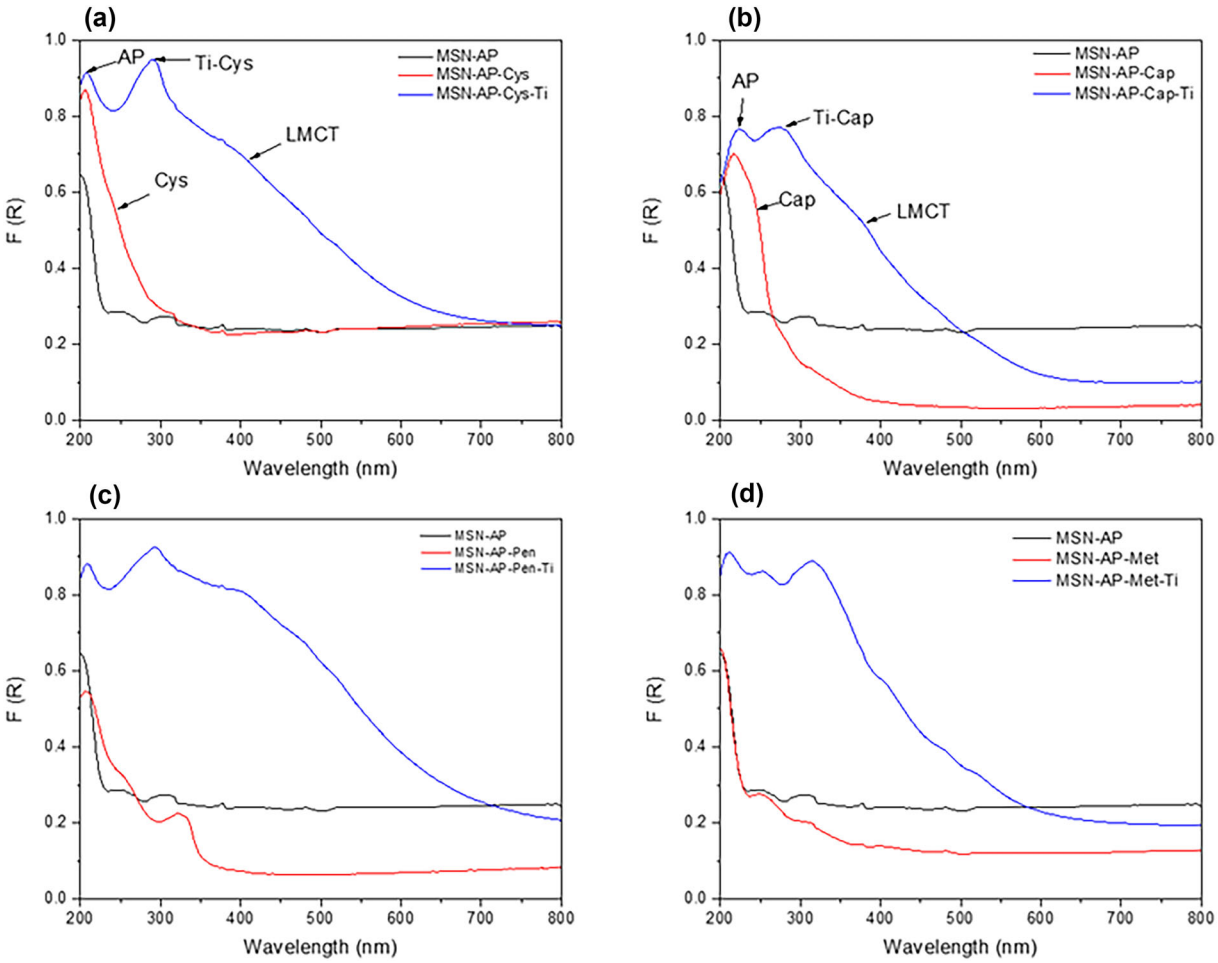

FIGURE 1 Diffuse reflectance UV/Vis solid absorption spectra of the functionalized systems.

and deformations of the silanol groups (Si–OH), respectively. Moreover, characteristic signals appear at 1084 and 460 cm^{-1}, representing the vibration of Si–O–Si bonds, alongside a 1643 cm^{-1} band linked to the deformation of adsorbed H_2O molecules.

In the spectra of the functionalized materials, additional bands emerge because of the integration of ligands and the organometallic complex.[27] Notably, N-H vibrations are observable in the range of 2952–2972 cm^{-1}, whereas their stretching frequencies are within 1379–1384 cm^{-1}. Additionally, the spectra exhibit weak intensity bands indicative of aliphatic and aromatic C–H stretching at approximately 2930 cm^{-1}. Bands at around 1600 cm^{-1}, attributed to the cyclopentadienyl ligands and amido groups, often overlap with signals from physiosorbed water.[27] Moreover, the functionalized systems manifest a faint signal at roughly 700 cm^{-1}, attributed to Si–C vibrations. These spectroscopic findings align with prior studies examining similar materials.[28–30]

3.4 | Powder X-ray diffraction studies

The selected materials underwent characterization via low-angle powder X-ray diffraction (XRD). The diffractograms exhibited characteristic reflections typical of hexagonally ordered mesoporous materials, as illustrated in Figure S2 for both MSN and its modified forms. Across the four nanomaterials, distinct patterns emerged at low 2θ values, with a prominent peak attributed to the 100 Miller plane. The unmodified MSN exhibited this peak at 2.23°, whereas its functionalized counterparts—MSN-AP, MSN-AP-Pen, and MSN-AP-Pen-Ti—showed variations at 2.46°, 2.41°, and 2.24°, respectively.

A notable observation was the decrease in peak intensities observed from the unmodified MSN to the titanocene-functionalized materials. Although the overall pattern persisted post-functionalization, the partial occlusion of the dispersion points within the porous system, owing to the incorporation of organic and/or organometallic fragments, resulted in a reduction in intensity.

Importantly, the peak position remained relatively stable post-functionalization, signifying the successful incorporation of different ligands into the MSN framework, consistent with prior research findings.[23,27–29]

These systems could be indexed as possessing a hexagonal lattice structure, evidenced by specific *d*-spacing values: 39.53 Å for MSN, 35.85 Å for MSN-AP, 36.64 Å for MSN-AP-Pen, and 14.77 Å for MSN-AP-Pen-Ti (see Table 1).

3.5 | X-ray fluorescence studies

The quantification of sulfur, silicon, and titanium was conducted via X-ray fluorescence analysis (Table 2). Evaluation of the sulfur content post-amino acid incorporation revealed varying percentages across materials. Specifically, MSN-AP-Cap exhibited a higher % S wt. (approximately 0.70%) compared with its counterparts, MSN-AP-Pen, MSN-AP-Cys, and MSN-AP-Met, which contained 0.50%, 0.40%, and 0.05% S wt., respectively. This discrepancy in sulfur content suggests that not all amino acid ligands are covalently attached to the material.

Further analysis of % wt. S in the materials following functionalization with the organometallic compound displayed a substantial decrease, particularly notable in MSN-AP-Cap-Ti (approximately 0.47%) and MSN-AP-Pen-Ti (approximately 0.32%). This observation indicates the possible removal of some amino acid moieties absorbed in the material during successive washing steps post-reaction. Consequently, only the sulfur from covalently bound amino acids appears to remain in the nanostructured systems.

It is important to note that the % S wt. of MSN-AP-Cys-Ti is surprisingly higher than that of MSN-AP-Cys. This can be explained by a decrease rather than an increase in the S:Si ratio of the materials (1:36 vs. 1:33 for MSN-AP-Cys vs. MSN-AP-Cys-Ti) in comparison with the other corresponding pairs where the trend is inverted.

Interestingly, the % S wt. of MSN-AP-Met is significantly lower than the other analogs. This is most probably due to the difference in the molecular structure of the amino acid moieties as methionine contains a thione rather than thiol, which is the functional group present in the other amino acids. This thione group may cause steric hindrance in the methionine molecule making its adsorption on the surface of the silica materials difficult, hence the low % S wt. In addition, the % S wt. in MSN-AP-Met-Ti is higher (3.15%) than in MSN-AP-Met, because of the presence of S-containing mercaptopropyl ligand.

The titanocene functionalization reactions targeted a theoretical range of 4–5 wt% Ti (Ti/SiO_2) for MSN-AP-Cys, MSN-AP-Cap, MSN-AP-Pen, and 10% Ti (Ti/SiO_2) for MSN-AP-Met-Ti. X-ray fluorescence analysis revealed the observed wt% Ti for the functionalized materials—1.45% for MSN-AP-Cys, 2.29% for MSN-AP-Cap, 1.25% for MSN-AP-Pen, and notably, 3.02% for MSN-AP-Met-Ti (refer to Table 2).

TABLE 1 XRD data of some MSN materials.

Material	*hkl*	2θ (°)	d_{hkl} (Å)	a_o (Å)
MSN	100	2.23	39.53	45.65
MSN-AP	100	2.46	35.85	41.40
MSN-AP-Pen	100	2.41	36.64	42.31
MSN-AP-Pen-Ti	100	2.24	39.50	45.61

TABLE 2 XRF and TG results.

Material	% S[a]	% Ti[a]	S:Ti ratio[a]	% AP[b]	% AA[b]
MSN-AP	-	-		14.56	-
MSN-AP-Cys	0.40	-		-	4.57
MSN-AP-Cap	0.70	-		-	15.57
MSN-AP-Pen	0.50	-		-	2.70
MSN-AP-Met	0.05	-		-	1.05
MSN-AP-Cys-Ti	0.48	1.45	1:3	-	n.a.
MSN-AP-Cap-Ti	0.47	2.29	1:2	-	n.a.
MSN-AP-Pen-Ti	0.32	1.25	1:2	-	n.a.
MSN-AP-Met-Ti	3.15	3.02	n.a.	-	n.a.

Abbreviations: AA, amino acids; n.a., not analyzed.

[a]Determined by XRF.

[b]Determined by TG.

Remarkably, the highest titanium incorporation occurred in MSN-AP-Met-Ti, attributable to the use of a higher theoretical percentage of Ti (Ti/SiO_2) in the functionalization process. This heightened functionalization aligns with previous studies from our group on ordered mesoporous silica materials, which revealed a maximum loading of metallocene complexes on MSN at approximately 2% of metal, despite starting with Ti/SiO_2 ratios of up to 5%.[30] This limited functionalization was ascribed to surface saturation and the weak basicity of both chloride atoms in the titanocene complex and the Si–OH groups of mesoporous silica.[30]

Notably, the S:Ti ratio approximated 1:2 across all titanocene-functionalized systems, indicating the direct binding of some titanocene moieties to the surface of the silica materials, in addition to those bound to S-containing ligands, as depicted in Scheme 1.

3.6 | NMR studies

The ^{13}C CP MAS NMR spectra of MSN-AP-Cap-Ti, MSN-AP-Pen-Ti, and MSN-AP-Met-Ti are shown in Figure 2. The spectrum of captopril-functionalized material MSN-AP-Cap-Ti shows clearly defined peaks at −1.78, 8.72, 20.21, 28.80, and 40.90 ppm, which were assigned to the functional groups, CH_3, CH_2-Si, CH_2-S, CH_2-CH_2, and CH_2-N, respectively. In addition, two signals at 58.13 and 172.44 ppm corresponding to the carbon atoms of the ethoxide (CH_3-CH_2-O-) and carbonyl (C=O) groups, respectively, were observed. Two sets of signals appeared at 127.25 and 141.86 ppm and were assigned to the carbon atoms of the cyclopentadienyl ring.

Similarly, the ^{13}C CP MAS NMR spectrum of MSN-AP-Pen-Ti showed six signals between 0 and 50 ppm attributed to the aliphatic carbon atoms of the aminopropyl-captopril chain. Furthermore, low-intensity signals between 128 and 143 ppm were assigned to the cyclopentadienyl moiety present in the material. The signals of the C atoms corresponding to the ethoxide and carbonyl groups were observed at 61.43 and 175.67 ppm, respectively. The ^{13}C CP MAS NMR spectrum of MSN-AP-Met-Ti showed somewhat similar chemical shifts with a set of broad bands between 0 and 50 ppm assigned to the aliphatic carbon atoms of the aminopropyl-methionine and mercaptopropyl moieties. In addition,

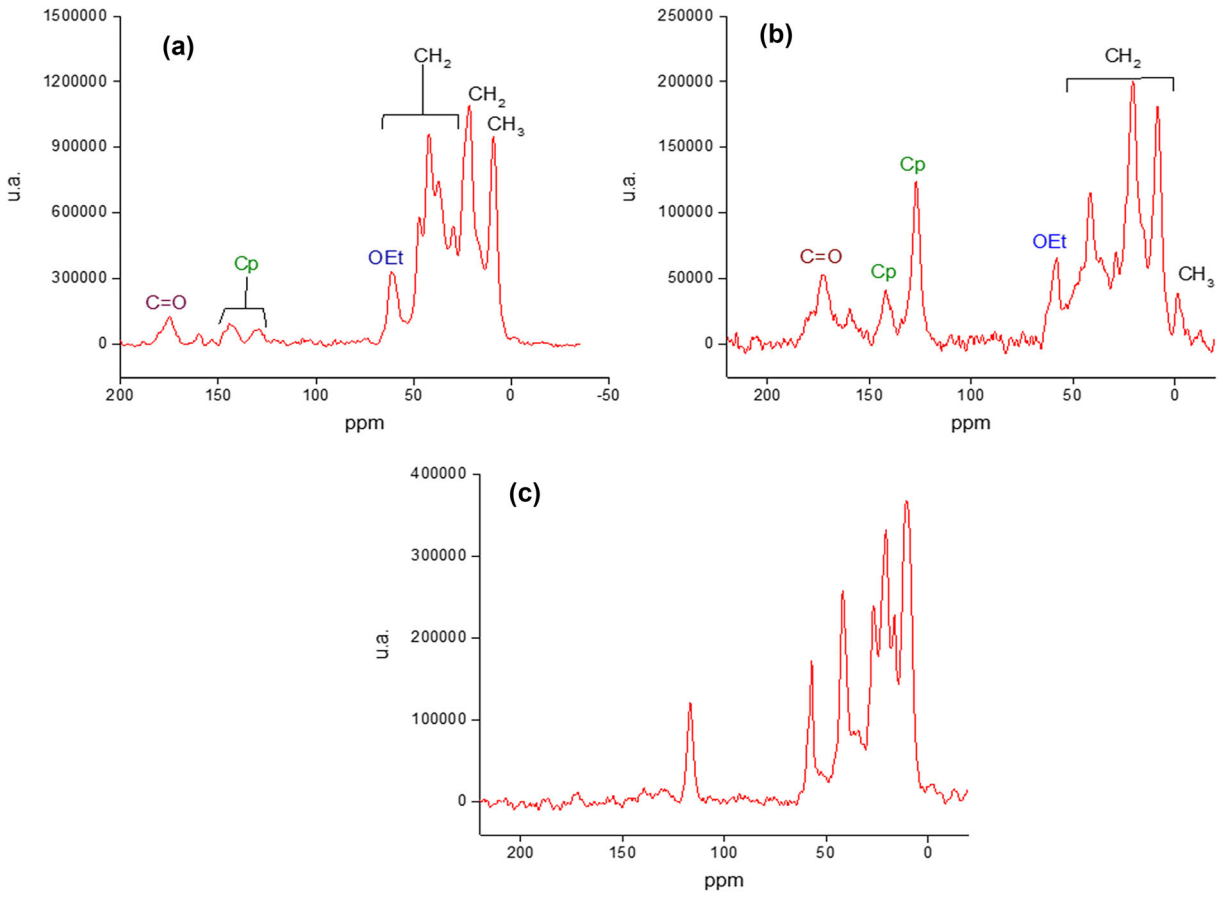

FIGURE 2 ^{13}C CP MAS NMR spectra of MSN-AP-Cap-Ti (a), MSN-AP-Pen-Ti (b), and MSN-AP-Met-Ti (c).

two signals of medium intensity at approximately 56 and 116 ppm correspond to the carbon atoms of the pendant ethoxide group and cyclopentadienyl ring, respectively, whereas the low-intensity signal at approximately 172 ppm is attributed to the carbon atom of the carbonyl group. The results herein are in line with earlier findings by our group for similar kinds of silica-based nanostructured materials functionalized with metallodrugs.[23,31]

Additionally, $^{47/49}$Ti NMR spectroscopy was used to determine the chemical environment around the Ti centre.[32,33] Although a potential correlation of the $^{47/49}$Ti MAS NMR resonances with the groups attached to the metal center in titanium (IV) precursors may be possible,[34] the two titanium isotopes present resonances only separated 22 Hz; with relatively strong quadrupole moments caused by the electric field gradients created by the electronic load within the different Ti distorted bonds and angles in both titanium environments for each polymorph observing only the "central transition" (+1/2----1/2) when the titanium nucleus is not in a symmetrical surrounding. This induces titanium atoms to experience a strong gradient field, which difficulted the interpretation of the signals. Thus, the $^{47/49}$Ti CP MAS NMR spectra of MSN-AP-Cap-Ti, MSN-AP-Pen-Ti, and MSN-AP-Met-Ti presented in Figure 3 showed very broad signals with different intensities, confirming the incorporation of titanium in the material and revealing some differences in the metal environment in each case as expected because of the potential different interactions of titanium with the different studied amino acids, the silica surface, and the thiolate ligand in the case of MSN-AP-Met-Ti.

3.7 | Electronic microscopy studies

The characterization of the materials also involved TEM analysis, with morphology and nanoparticle size assessed using the ImageJ® program.[35] The TEM examination (Figures 4a and b) depicted the materials as quasi-spherical in morphology, exhibiting a hexagonally ordered pore distribution. The TEM images clearly showcased the internal pore distribution and parallel channels traversing the entire mesoporous particle.

Analysis using ImageJ revealed that the original MSNs measured 144 ± 4 nm in particle size, whereas the final materials, such as MSN-AP-Cys-Ti, measured 142 ± 2 nm. These results suggest that the structural features and parameters of the nanoparticles remained largely unaffected by the functionalization processes.

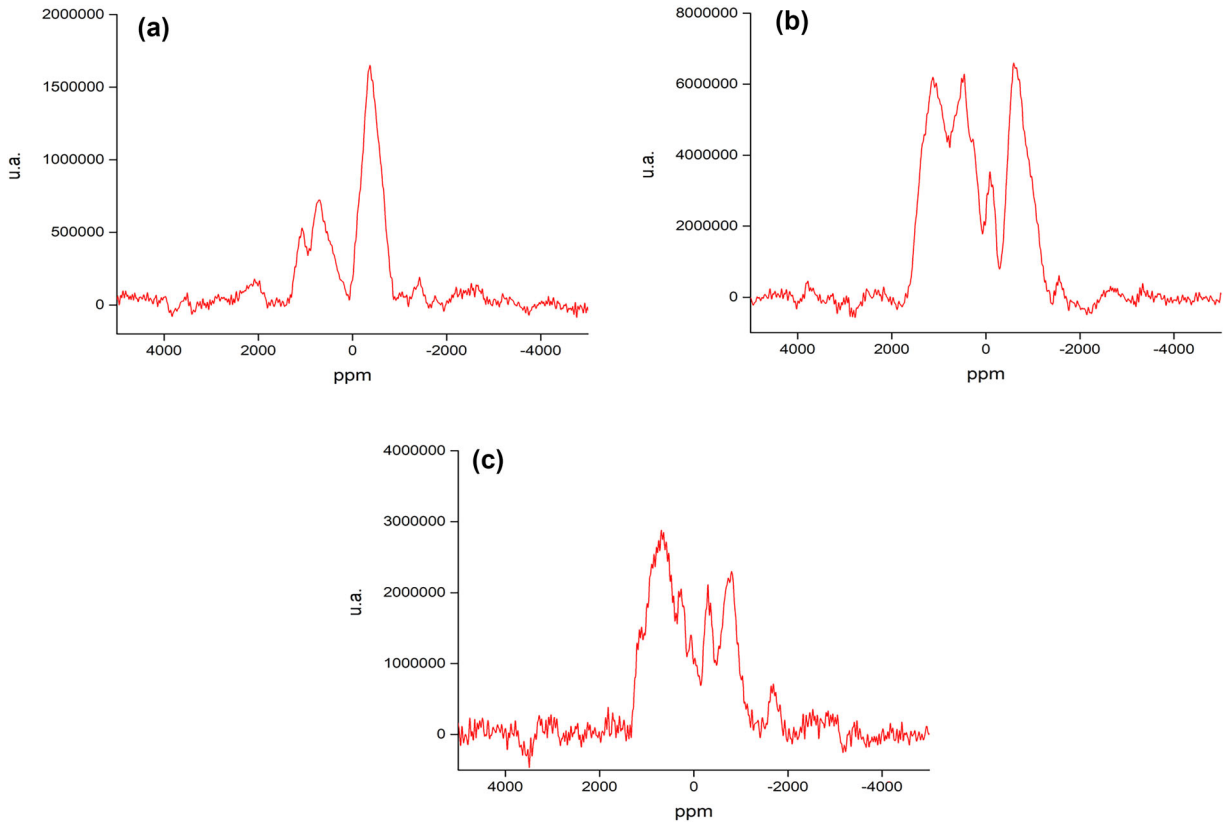

FIGURE 3 $^{47/49}$Ti NMR spectra of MSN-AP-Cap-Ti (a), MSN-AP-Pen-Ti (b), and MSN-AP-Met-Ti (c).

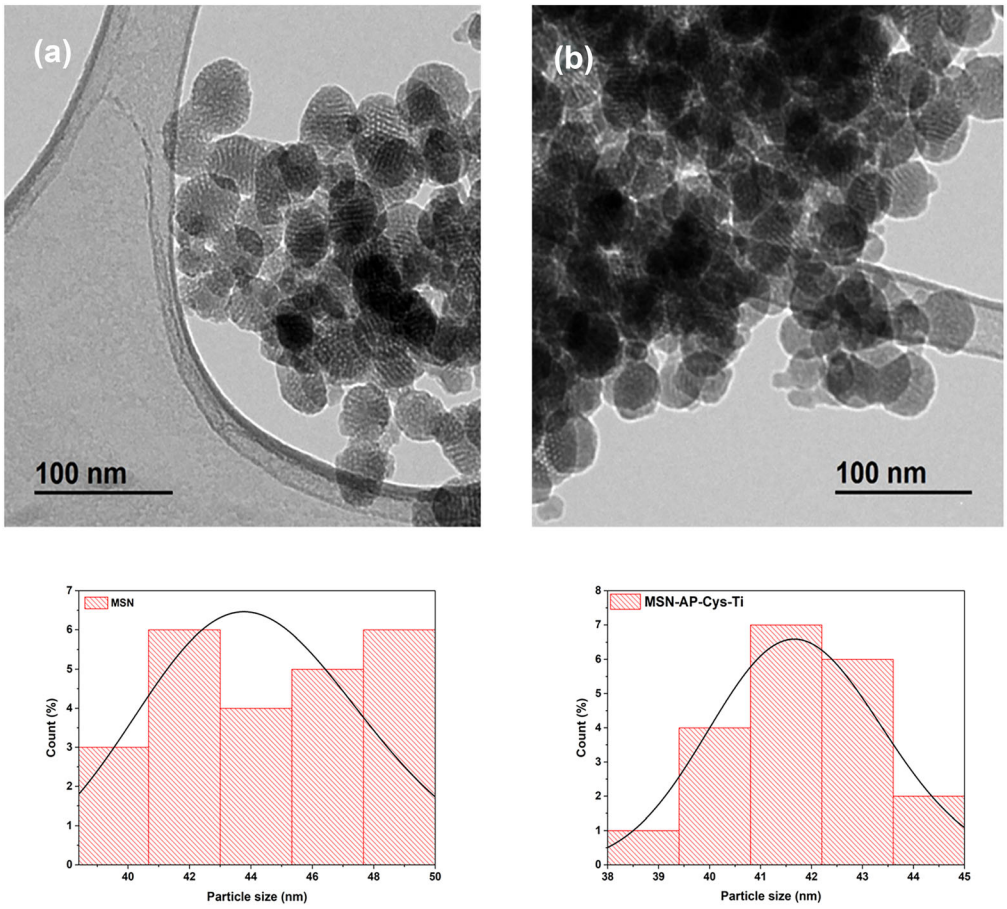

FIGURE 4 TEM images of MSN (a) and MSN-AP-Cys-Ti (b) with their corresponding histograms.

This consistency aligns with earlier findings from our group.[23]

The material with a high content of Ti (MSN-AP-Cap-Ti) was also analyzed by STEM (Figure 5), in order to observe the different elements in the functionalized silica. The STEM images of MSN-AP-Cap-Ti show that the organic fragments (AP ligand and captopril) and the titanium complex in the silica are homogeneously distributed throughout the nanomaterial.

3.8 | Thermogravimetric studies

The quantification of the AP and amino acid ligands was conducted through thermoanalyses, observing weight loss between 125 and 650°C (Figure S3), which demonstrated the thermal stability of these nanostructured systems. The incorporation of AP resulted in a 14.56% wt., whereas cysteine, captopril, penicillamine, and methionine showed % wt. values of 4.57%, 15.57%, 2.70%, and 1.05%, respectively (Table 2). These findings align with X-ray fluorescence studies indicating a higher captopril integration into the silica material compared with other amino acids. This trend is consistent with similar ligands, such as mercaptopropyl-based systems loaded into silica-based nanostructured materials.[31]

3.9 | Qualitative DNA interaction studies

The mechanism of action of titanocene derivatives has established DNA as one of their potential biological targets.[36] Accordingly, to model the behavior of these systems with DNA, absorption spectra were recorded for free DNA and the material MSN-AP-Cap-Ti at various interaction times. This experimental setup aimed to simulate and analyze the interaction dynamics between the material and DNA.

Figure 6 shows that the absorbance of DNA decreased significantly on interaction with the studied metallodrug nanosystem. Additionally, a very slight blue shift of the peaks (hypsochromic effect) indicates adsorption of DNA on the surface of the particles forming DNA adducts, a phenomenon previously reported.[37,38] In addition,

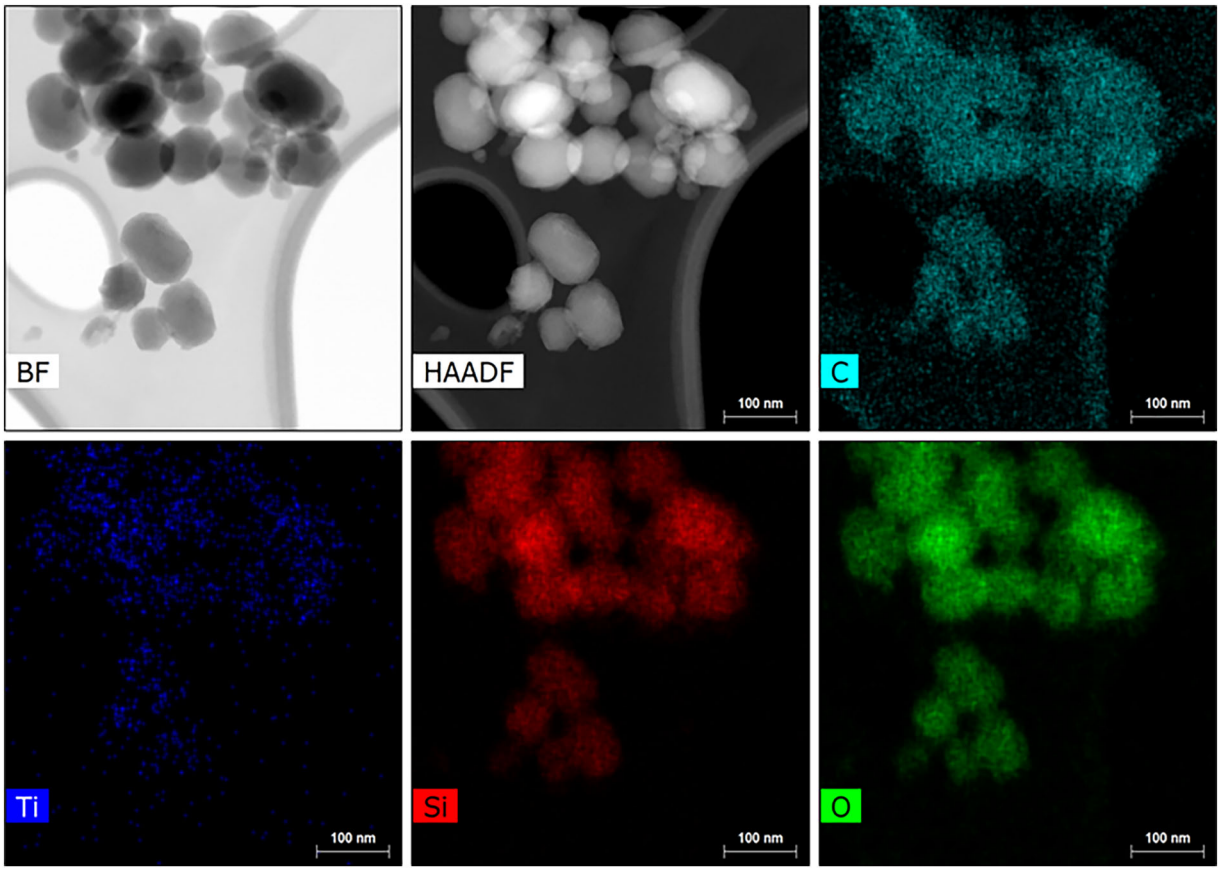

FIGURE 5 Bright field (BF), high-angle annular dark-field (HAADF) Scanning Transmission Electron Microscopy (STEM) image of MSN-AP-Cap-Ti and mapping of C (cyan), Ti (blue), Si (red), and O (green), as labeled in the different micrographs.

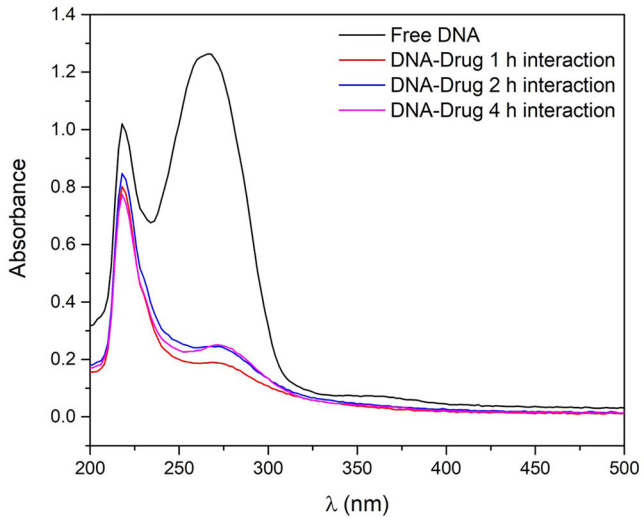

FIGURE 6 DNA binding study of MSN-AP-Cap-Ti.

electrostatic interactions between MSN-AP-Cap-Ti and DNA are proposed to be responsible for the adsorption of DNA, so this could be one of the main targets, thus producing cell apoptosis.

3.10 | Cytotoxicity tests

The cytotoxic ability of the silica-based materials, MSN-AP-Cys-Ti, MSN-AP-Cap-Ti, MSN-AP-Pen-Ti, and MSN-AP-Met-Ti, was determined by an MTT study in the breast cancer cell line MDA-MB-231, comparing the cytotoxicity with the healthy cell line Hek-293T. The percentage viability of the materials in both cell lines is presented in Figures 7 and 8.

For the breast cancer cell line (MDA-MB-231), cell viability dependence on the concentration of the materials can be clearly observed, with the materials with cysteine (MSN-AP-Cys-Ti) and captopril (MSN-AP-Cap-Ti) being the most active in terms of IC_{50} with respect to the concentration of the material (Table 3, left column for each cell line). However, when these concentrations are recalculated in terms of titanium loading (cytotoxic agent), a similar activity was observed amongst the materials MSN-AP-Cys-Ti, MSN-AP-Cap-Ti, and MSN-AP-Pen-Ti (Table 3, right column for each cell line).

Interestingly, MSN-AP-Met-Ti has the highest IC_{50} having the highest titanium content (3.09%) but the lowest content of amino acid (see Table 2), which is known

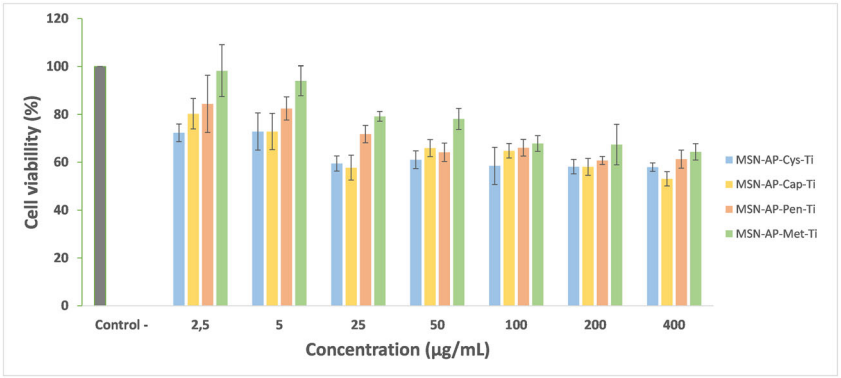

FIGURE 7 MTT viability assay of MDA-MB-231 cells after incubation with the materials. The results are expressed as % of retained viability in comparison with the negative control (mean ± SD, 3 replicates, $p < 0.05$).

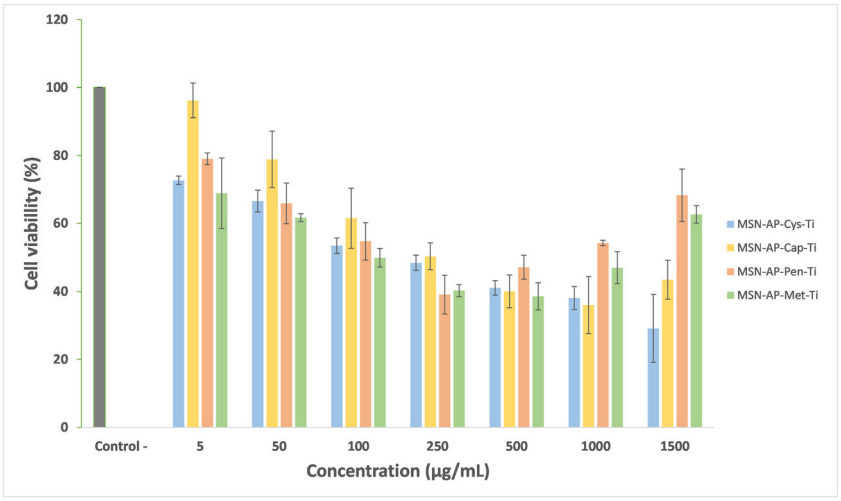

FIGURE 8 MTT viability assay of Hek-293T cells after incubation with the materials. The results are expressed as % of retained viability in comparison with the negative control (mean ± SD, 3 replicates, $p < 0.05$).

TABLE 3 Cytotoxic activity with standard deviation and its reference as a function of metal content [M].

	MDA-MB-231		Hek293T	
Material	**IC_{50} (µg/mL)**	**IC_{50} [M] (µg/mL)**	**IC_{50} (µg/mL)**	**IC_{50} [M] (µg/mL)**
MSN-AP-Cys-Ti	618.37 ± 72.25	8.97 ± 1.65	203.55 ± 72.27	2.95 ± 1.05
MSN-AP-Cap-Ti	521.69 ± 62.90	11.95 ± 1.44	258.57 ± 60.31	5.92 ± 1.38
MSN-AP-Pen-Ti	1004.80 ± 67.72	12.56 ± 1.55	145.38 ± 64.53	1.82 ± 0.81
MSN-AP-Met-Ti	1335.42 ± 70.36	40.33 ± 1.61	203.55 ± 73.17	6.15 ± 2.21

that could be important in the cell internalization process. Therefore, for this material, it seems that the titanium amount is crucial for enhancing the cytotoxic activity compared with the other systems. Therefore, from the results in the MDA-MB-231 cell line, in materials with cysteine, captopril, and penicillamine MSN-AP-Cys-Ti, MSN-AP-Cap-Ti, and MSN-AP-Pen-Ti, titanium activity is linked to incorporation through the amino acid, creating a synergy that enhances cell internalization and therefore the cytotoxic activity of these functionalized nanosystems, although the amino acid quantity does not seem to have a critical role in MSN-AP-Met-Ti that has incorporated titanium centers through the interaction with the mercaptopropyl ligand rather than with the methionine.

Analyzing the cell viability in the Hek-293T line, the materials functionalized with titanium through the amino acid are only slightly more active than MSN-AP-Met-Ti. It is important to note that higher cytotoxicity was observed for the materials for the healthy cell line Hek-293T with IC_{50} values being lower than those recorded for cancer cells.

In summary, considering the good stability of the systems in solution, which do not release metal-containing species as confirmed by the absence of signals of titanium species in the DNA-binding studies, which validate the action of these materials as non-classical drug-delivery systems,[39] these results confirm the stability of the materials as well as their selectivity, which is why it has great

potential to carry out future in vivo trials and could be a great step for new treatments based on chemotherapy.[40]

4 | CONCLUSIONS

Four novel metallodrug functionalized nanostructured materials incorporating four different amino acids, MSN-AP-Cys-Ti, MSN-AP-Cap-Ti, MSN-AP-Pen-Ti, and MSN-AP-Met-Ti, have been prepared and characterized. It was observed that the incorporation of the amino acids and titanocene dichloride took place mainly inside the pores of the MSN-based systems, with MSN-AP-Met-Ti showing the highest amount of titanium when compared with the other materials. This may be ascribed to the fact that MSN-AP-Met-Ti was prepared following a different synthetic procedure, namely, incorporating first the amino acid to the silica through the AP ligand followed by functionalization with the titanocene covalently bound to the MP ligand. In addition, qualitative DNA binding studies carried out on MSN-AP-Cap-Ti indicated the possible formation of DNA adducts via adsorption of the DNA on the surface of the metallodrug functionalized nanomaterials.

The cytotoxicity of the materials was evaluated by an MTT study in the breast cancer cell line MDA-MB-231 and compared with the healthy cell line Hek-293T. The materials with cysteine, captopril, and penicillamine were observed to be the most active in terms of IC_{50} with respect to the concentration of the functionalized material or titanium loading. Interestingly, these materials, MSN-AP-Cys-Ti, MSN-AP-Cap-Ti, and MSN-AP-Pen-Ti, have a higher amino acid incorporation than MSN-AP-Met-Ti. This may infer that titanium activity is linked to incorporation through the amino acid, creating a synergy that enhances cell internalization and therefore the cytotoxic activity of these functionalized nanosystems.

Considering that MDA-MB-231 is a highly aggressive breast cancer cell line,[40] the cytotoxicity demonstrated by these new functionalized materials reported here makes them a promising starting point in developing and optimizing the selectivity of therapeutic nanosystems functionalized with both amino acids and different kinds of titanocene compounds for the search of alternative therapeutic agents based on metals different than platinum.

AUTHOR CONTRIBUTIONS

Michael Aondona Iorhemba: Conceptualization; methodology; software; investigation; writing—original draft; writing—review and editing; visualization; project administration. **Karina Ovejero-Paredes:** Methodology; software; formal analysis; investigation; data curation. **Diana Díaz-García:** Methodology; software; investigation; formal analysis; data curation; writing—original draft; writing—review and editing; visualization; supervision. **Victoria García-Almodóvar:** Investigation; formal analysis. **Sulaiman Ola Idris:** Conceptualization; methodology; resources; funding acquisition; supervision. **Gideon Adamu Shallangwa:** Conceptualization; methodology; resources; funding acquisition; supervision. **Ibrahim Abdulkadir:** Methodology; validation; supervision. **José M. Méndez-Arriaga:** Formal analysis; investigation; data curation; writing—original draft; writing—review and editing; visualization. **Sanjiv Prashar:** Data curation; writing—original draft; writing—review and editing. **Marco Filice:** Validation; resources; data curation; visualization; writing—review and editing. **Santiago Gómez-Ruiz:** Conceptualization; validation; resources; data curation; writing—original draft; writing—review and editing; funding acquisition; visualization; supervision; project administration.

ACKNOWLEDGMENTS

We would like to thank funding from the research project PID2022-136417NB-I00 financed by MCIU/AEI/10.13039/501100011033/ and "ERDF A way of making Europe," and from the Research Thematic Network RED2022-134091-T financed by MCIU/AEI/10.13039/501100011033. TETFUND is gratefully acknowledged for the mobility grant (M.A.I.). The authors would also like to thank the Universidad Rey Juan Carlos for the support of our research group COMET-NANO through the project M3271, the Ahmadu Bello University, and Federal University of Agriculture for their support. Part of this research work was funded by the Instituto de Salud Carlos III (ISCIII) (projects No.: DTS20/00109 [AES 2020] and PI22/00789 [AES 2022]) and by the Ministerio de Ciencia e Inovación (MCIN/AEI) (project No.: CPP2022-009952, MCIN/AEI/10.13039/501100011033, also funded by European Union NextGenerationEU/PRTR).

CONFLICT OF INTEREST STATEMENT

The authors declare no conflict of interest.

DATA AVAILABILITY STATEMENT

All data are available on request.

ORCID

Michael Aondona Iorhemba https://orcid.org/0000-0003-2590-0219
Karina Ovejero-Paredes https://orcid.org/0000-0002-5296-2696
Diana Díaz-García https://orcid.org/0000-0003-3057-4905
Victoria García-Almodóvar https://orcid.org/0000-0003-2609-7683

Sulaiman Ola Idris https://orcid.org/0000-0002-0199-5121
Gideon Adamu Shallangwa https://orcid.org/0000-0002-0700-9898
Ibrahim Abdulkadir https://orcid.org/0000-0002-4025-1889
José M. Méndez-Arriaga https://orcid.org/0000-0002-7337-6071
Sanjiv Prashar https://orcid.org/0000-0002-6588-878X
Marco Filice https://orcid.org/0000-0001-8142-4566
Santiago Gómez-Ruiz https://orcid.org/0000-0001-9538-8359

REFERENCES

[1] IARC Working Group on the Evaluation of Cancer-Preventive Strategies, International Agency for Research on Cancer, World Health Organization, *Cervix cancer screening*, Vol. 10, Diamond Pocket Books (P) Ltd **2005**.
[2] W. A. Wani, S. Prashar, S. Shreaz, S. Gomez-Ruiz, *Coord. Chem. Rev.* **2016**, *312*, 67.
[3] M. Pineros, L. Mery, I. Soerjomataram, F. Bray, E. Steliarova-Foucher, *JNCI* **2021**, *113*(1), 9.
[4] G. N. Sharma, R. Dave, J. Sanadya, P. Sharma, K. Sharma, *J. Adv. Pharmaceut. Technol. Res.* **2010**, *1*(2), 109.
[5] A. Kamath Mulki, M. Withers, *BMC Women's Health* **2021**, *21*(1), 1.
[6] A. G. Waks, E. P. Winer, *Jama* **2019**, *321*(3), 288.
[7] V. Schirrmacher, *Int. J. Oncol.* **2019**, *54*(2), 407.
[8] B. Rosenberg, L. VanCamp, *Cancer Res.* **1970**, *30*(6), 1799.
[9] U. Ndagi, N. Mhlongo, M. E. Soliman, *Drug des. Devel. Ther.* **2019**, *11*, 599.
[10] K. D. Mjos, C. Orvig, *Chem. Rev.* **2014**, *114*(8), 4540.
[11] Y. Ellahioui, S. Prashar, S. Gomez-Ruiz, *Inorganics* **2017**, *5*(1), 4.
[12] Y. Ellahioui, S. Prashar, S. Gomez-Ruiz, *Curr. Med. Chem.* **2016**, *23*(39), 4450.
[13] M. Poursharifi, M. T. Wlodarczyk, A. J. Mieszawska, *Inorganics* **2018**, *7*(1), 2.
[14] T. Kiss, É. A. Enyedy, T. Jakusch, *Coord. Chem. Rev.* **2017**, *352*, 401.
[15] S. Attoub, A. M. Gaben, S. Al-Salam, M. A. H. Al Sultan, A. John, M. G. Nicholls, G. Petroianu, *Ann. N. Y. Acad. Sci.* **2008**, *1138*(1), 65.
[16] S. J. Chen, C. C. Kuo, H. Y. Pan, T. C. Tsou, S. C. Yeh, J. Y. Chang, *Biochem. Pharmacol.* **2015**, *95*(1), 28.
[17] V. D. Bonifácio, S. A. Pereira, J. Serpa, J. B. Vicente, *Br. J. Cancer* **2021**, *124*(5), 862.
[18] C. Amgoth, S. Joshi, *Mater. Res. Express* **2017**, *4*(10), 105306.
[19] Z. Li, Y. Zhang, N. Feng, *Expert Opinion Drug Deliv.* **2019**, *16*(3), 219.
[20] R. K. Kankala, Y. H. Han, J. Na, C. H. Lee, Z. Sun, S. B. Wang, T. Kimura, Y. S. Ok, Y. Yamauchi, A. Z. Chen, K. C. Wu, *Adv. Mater.* **2020**, *32*(23), 1907035.
[21] B. Cho, *Mater. Res. Express* **2019**, *6*(4), 045016.
[22] C. R. P. Silva, F. da Rocha Ferreira, G. D. Webler, A. O. S. da Silva, F. C. de Abreu, E. J. Fonseca, *Mater. Res. Express* **2017**, *4*(6), 065402.
[23] D. Díaz-García, E. Fischer-Fodor, C. I. Vlad, J. M. Méndez-Arriaga, S. Prashar, S. Gómez-Ruiz, *Microporous Mesoporous Mater.* **2021**, *323*, 111238.
[24] I. Del Hierro, Y. Pérez, P. Cruz, R. Juárez, *Eur. J. Inorg. Chem.* **2017**, *24*, 3030.
[25] J. Karges, D. Díaz-García, S. Prashar, S. Gómez-Ruiz, G. Gasser, *ACS Appl. Bio Mater.* **2021**, *4*(5), 4394.
[26] M. Kobayashi, V. Petrykin, K. Tomita, M. Kakihana, *J. Ceram. Soc. Jpn.* **2008**, *116*(1352), 578.
[27] S. Gómez-Ruiz, A. García-Peñas, S. Prashar, A. Rodríguez-Diéguez, E. Fischer-Fodor, *Materials* **2018**, *11*(2), 224.
[28] I. Del Hierro, S. Gómez-Ruiz, Y. Pérez, P. Cruz, S. Prashar, M. Fajardo, *Dalton Trans.* **2018**, *47*(37), 12914.
[29] D. Pedraza, J. Díez, M. Colilla, M. Vallet-Regí, *Biomed. Glass.* **2018**, *4*(1), 1.
[30] D. Pérez-Quintanilla, S. Gómez-Ruiz, Ž. Žižak, I. Sierra, S. Prashar, I. del Hierro, M. Fajardo, Z. D. Juranić, G. N. Kaluđerović, *Chem.–a Eur. J.* **2009**, *15*(22), 5588.
[31] D. Díaz-García, K. Montalbán-Hernández, I. Mena-Palomo, P. Achimas-Cadariu, A. Rodríguez-Diéguez, E. López-Collazo, S. Prashar, K. Ovejero Paredes, M. Filice, E. Fischer-Fodor, S. Gómez-Ruiz, *Pharmaceutics* **2020**, *12*(6), 512.
[32] D. Padro, A. P. Howes, M. E. Smith, R. Dupree, *Solid State Nucl. Magn. Reson.* **2020**, *15*(4), 231.
[33] D. Padro, V. Jennings, M. E. Smith, R. Hoppe, P. A. Thomas, R. Dupree, *J. Phys. Chem. B* **2002**, *106*(51), 13176.
[34] R. Ballesteros, M. Fajardo, I. Sierra, C. Force, I. del Hierro, *Langmuir* **2009**, *25*(21), 12706.
[35] ImageJ, National Institutes of Health, USA. https://imagej.nih.gov/ij/
[36] A. García-Peñas, S. Gómez-Ruiz, D. Pérez-Quintanilla, R. Paschke, I. Sierra, S. Prashar, I. del Hierro, G. N. Kaluđerović, *J. Inorg. Biochem.* **2012**, *106*(1), 100.
[37] M. Cini, T. D. Bradshaw, S. Woodward, *Chem. Soc. Rev.* **2017**, *46*(4), 1040.
[38] A. Kathiravan, R. Renganathan, *Polyhedron* **2009**, *28*(7), 1374.
[39] D. Díaz-García, S. Prashar, S. Gómez-Ruiz, *Int. J. Mol. Sci.* **2023**, *24*(3), 2332.
[40] E. Chang, S. S. Mougalian, K. B. Adelson, M. R. Young, J. B. Yu, *Breast Cancer Res. Treat.* **2019**, *173*(1), 209.

SUPPORTING INFORMATION

Additional supporting information can be found online in the Supporting Information section at the end of this article.

How to cite this article: M. A. Iorhemba, K. Ovejero-Paredes, D. Díaz-García, V. García-Almodóvar, S. O. Idris, G. A. Shallangwa, I. Abdulkadir, J. M. Méndez-Arriaga, S. Prashar, M. Filice, S. Gómez-Ruiz, *Appl Organomet Chem* **2024**, *38*(6), e7483. https://doi.org/10.1002/aoc.7483